RC25429 (WAT1311-151) November 19, 2013
Physics

IBM Research Report

Plasma-Enhanced Chemical Vapor Deposition (PECVD): Silicon Nitride Films

Deborah Neumayer
IBM Research Division
Thomas J. Watson Research Center
P.O. Box 208
Yorktown Heights, NY 10598
USA

Research Division
Almaden - Austin - Beijing - Cambridge - Haifa - India - T. J. Watson - Tokyo - Zurich

LIMITED DISTRIBUTION NOTICE: This report has been submitted for publication outside of IBM and will probably be copyrighted if accepted for publication. It has been issued as a Research Report for early dissemination of its contents. In view of the transfer of copyright to the outside publisher, its distribution outside of IBM prior to publication should be limited to peer communications and specific requests. After outside publication, requests should be filled only by reprints or legally obtained copies of the article (e.g., payment of royalties). Copies may be requested from IBM T. J. Watson Research Center , P. O. Box 218, Yorktown Heights, NY 10598 USA (email: reports@us.ibm.com). Some reports are available on the internet at http://domino.watson.ibm.com/library/CyberDig.nsf/home .

Plasma-Enhanced Chemical Vapor Deposition (PECVD): Silicon Nitride Films

Deborah Neumayer

IBM Watson Research Center Yorktown Heights, NY, USA; dneu@us.ibm.

Keywords

Silicon nitride, PECVD, FTIR, stress, mechanism

Abstract

An overview of amorphous hydrogenated silicon nitride (a-SiN_x:H) prepared by plasma-enhanced chemical vapor deposition (PECVD) is discussed including applications, plasma deposition systems, characterization of films by FTIR, mechanism of film growth as determined by process chemistry, and dependence of film properties on process parameters.

Introduction

Amorphous hydrogenated silicon nitride (a-SiN_x:H) materials prepared by plasma-enhanced chemical vapor deposition (PECVD) are of high interest because of their suitability for diverse applications in many fields. There has been a growing interest in thin film dielectrics that can be deposited at low substrate temperatures less than 500^{o}C for many applications in many fields including microelectronics, photovltaics, and photonics. Thermal chemical vapor deposition of silicon nitride requires temperatures in excess of 600^{o}C in order to decompose ammonia.[1] The additional energy a plasma introduces enhances ammonia decomposition and enables deposition of silicon nitride at temperatures less than 500^{o}C. PECVD silicon nitride films are non-stoichiometric, and contain a substantial amount of hydrogen. The high hydrogen content results in a film that is actually a-SiN_x:H, instead of Si_3N_4. The non-stoichiometric nature of PECVD a-SiN_x:H allows tailoring of film properties including stress, optical properties such as refractive index, uv absorption, passivation behavior, and etch resistance. Plasma enhanced chemical vapor deposited silicon nitride films deposited at low temperatures have the advantages of low processing temperature, and uniform film deposition facilitating their use in a myriad of applications.

PECVD silicon nitride has been widely used in microelectronic device fabrication for many applications such as final passivation and mechanical protective layers for underlying circuits,[2] diffusion barriers against mobile ions and moisture,[3,4,5] masks for selective oxidation of silicon, [2] stop layers for both etch and chemical mechanical polishing (CMP) processes, [2] and protective films against Cu oxidation and diffusion. [2,11] PECVD silicon nitride is utilized as final passivation layers for GaAs devices.[6,7,8, 9] Plasma nitride films have been used as stop layers for dual Damascene processing.[10] In dual Damascence, trenches and via holes are etched in two separate steps into an interlayer dielectric, and then filled with metal to form wires and interlevel connections. The nitride layers are used to ensure that the trench depth is constant across a wafer, independent of variations in etch rate. Another important area of application of plasma deposited silicon nitride is for the gate dielectric in active-matrix liquid crystal displays (AMLCD's).[11] In AMLCDs, very low RF powers are employed, and a large hydrogen concentration (bonded to nitrogen) is desirable to ensure good stability of the interface with the amorphous silicon which forms the transistor active layer. PECVD silicon nitride is employed as the gate dielectric for amorphous silicon thin film transistors because of its good interfacial properties with

hydrogenated amorphous silicon (aSi:H).[12,13,14] PECVD nitride has been utilized as a gate dielectric for graphene.[15] Because of the low deposition temperatures which reduce thermal budget and film stress, PECVD SiN has enabled development of micro-opto-electro-mechanical (MOEMS) and microelectro-mechanical systems (MEMS) such as static membranes, tunable inductors, and vertical cavity surface emitting laser (VCSEL) and tunable MEMS Fabry–Perot (FP) optical filters on organic substrates.[16] In particular, devices involving air-gaps and suspended membranes—e.g. Fabry–Perot filter (FPF)—require a precise stress control for a successful implementation. Mechanical characteristics of the silicon nitride membrane, including the elastic modulus of the material and the intrinsic stress gradient through the thickness of the SiN*x* layer, are essential in ensuring structural integrity and filter performance.[17,18] Highly stressed SiN films deposited by plasma enhanced chemical vapor deposition (PECVD) have been utilized to introduce strain in an underlying silicon transistor channel. Substantial increase in transistor device speed has been achieved by application of these highly stressed SiN films, which in turn has been successfully incorporated into the dual stress liner (DSL) technology benefiting both *n*FET and *p*FET type of transistors in server microprocessors and consumer products.[19,20] One of the key technological advances in solar cell technology, has been the use of PECVD silicon nitride as an antireflection coating and as a surface and bulk passivation layer for both surface and bulk.[21,22, 23]

Plasma Systems

Industrial plasma systems for a-SiN_x:H deposition can be divided into two main groups: direct plasma systems with parallel plate electrodes where wafers are within the plasma zone and indirect plasma systems where wafers are outside the plasma zone. Direct plasma systems usually employ a showerhead configuration with a heated susceptor operating at from a few hundred mTorr to a few Torr and a radio frequency power of 13.56 MHz. Typically, the showerhead is the electrode and connected to the power supply while the susceptor is grounded. When the electric field is generated between the electrodes, atoms are ionized and release electrons. The electrons in the gas are accelerated by RF field and can ionize the gas directly or indirectly by collisions. Temperatures of 250 to 500^{o}C are typically employed. Direct (PECVD) of SiN typically utilizes SiH_4 with ammonia as the most common oxidant, although pure nitrogen is also used.

Remote plasma enhanced chemical vapor deposition (RPECVD) or indirect plasma deposition is characterized by the substrate placed outside of the plasma generation region and not all of the process gases are subjected to direct plasma excitation. The plasma generation regions and the areas of reactors used for substrate location are separated in space. Only some of the initial reagents are excited by direct collisions with accelerated electrons in the plasma generation regions, and these are then transported in the direction of the deposition zone. Other reactants are introduced downstream of the discharge generation region and can undergo indirect excitation. An immediate benefit is that the substrate is not subject to energetic ion bombardment. Another potential benefit is controlled excitation of reactants. The solar cell industry has embraced indirect plasma systems utilizing linear microwave plasma sources to provide low cost high throughput large area SiN plasma depositions.[24,25] The indirect microwave (2.45 GHz microwave (uW) frequency) plasma systems decouple the plasma from the wafer transportation system enabling use of wafers with arbitrary shape and size. Microwave plasmas have high charge carrier concentrations at low ion- and electron energies below 10 eV, which minimizes surface damage from ion bombardment.

Film Characterization

Silicon nitride has no fixed stoichiometry and film composition of PECVD a-SiN_x:H varies widely from nitrogen doped amorphous Si as x approaches 0 to nitrogen rich silicon nitride with $x > 1.33$. Silicon nitride films incorporate a considerable amount of hydrogen with hydrogen bonded as Si-H or N-

H. Infrared spectroscopy (IR) is one of the most useful techniques for detecting hydrogen atoms and obtaining information on their bonding configurations. IR gives direct characterization of both film composition and atomic structure. The frequency assignments of various Si-N network absorptions (1100-700 cm^{-1}), Si-H (2000-2200 cm^{-1}), and N-H (3300 cm^{-1}, 1550 cm^{-1} and 1175 cm^{-1} are summarized from literature in Table 1.

As shown in Figure 1(a) and 1(b), the FTIR spectrum of PECVD a-SiN_x:H films deposited from SiH_4 and NH_3 varies dramatically with the gas phase composition during growth. The NH_3 gas phase composition X_g is defined as the ratio between NH_3 and $SiH_4 + NH_3$ flow rates which is varied between 0 to 0.975. [26]

$$X_g = NH_3/(SiH_4 + NH_3) \qquad (1)$$

In Figure 1(a), as X_g is increased the absorption at 640 cm^{-1} attributed to Si-H rocking mode decreases and is no longer observed at $X_g > 0.8$, concurrently the absorption at 480cm^{-1} attributed to weak Si-N symmetric stretch appears and increases as X_g increases as $X_g > 0.8$. The absorption at 480 cm^{-1} attributed to weak Si-N symmetric stretch where N is bond to three Si atoms N-Si_3 and is referred to as the silicon "breathing mode". The symmetric breathing mode is normally infrared inactive but is likely made active by increasing nitrogen substitution and disruption of the Si-Si network. [26,27,28,29] Raman analysis of the spectral region 250-600 cm^{-1} provides evidence that the disorder in the silicon network increases as the nitrogen content increases.[30] The disorder is introduced via bond angle distortion in the Si-Si network and from silicon cluster formation in a-SiN_x:H films. [31,33,35] In Figure 1(a), as X_g is increased the absorption at 640 cm^{-1} decreases and is no longer observed at $X_g > 0.8$. The absorption at 640 cm^{-1} is attributed to Si-H rocking mode. The SiH rocking absorption is observed to decrease in intensity, broaden and shift to higher frequencies as the nitrogen content in silicon nitride is increased.[26,28, 32,33]

As X_g increases in Figure 1(a), the Si-N network absorptions found between 700 and 1100 cm^{-1} become stronger. The broad absorption between 700 and 1100 cm^{-1} is indicative of the overall disorder of the Si-N network and wide range of bond angle distortion. This absorption band is generally centered at ~840 cm^{-1} and is typically assigned to the asymmetric stretching of SiN, however the band can be deconvoluted into three peaks centered at ~780, ~840-870, and 900-1100 cm^{-1}.[26,29,30,32,34] The relative intensities of the deconvoluted peaks are dependent on the film stoichiometry and microstructure as discussed extensively in the literature.[26-43] The shoulder at 780 cm^{-1} disappears when $X_g > 0.2$ and is attributed to the stretching mode of an isolated Si-N bond where the N atom is bonded to three Si atoms and the Si atom is backbonded by three other Si atoms, a N-Si-(Si_3) configuration.[27] Not surprisingly, as nitrogen content of the film increases, the probability of a N-Si-(Si_3) configuration diminishes and the vibrational mode is no longer observed. The broad absorptions centered at ~840-870, and 900-1100 cm^{-1} are attributed to the Si-N assymetric stretch transverse (TO) and longitudinal optical (LO) modes at 840-870 cm^{-1} and 900-1100 cm^{-1} respectively.[26,28,35,36,37] The TO and LO modes arise from the reststrahlen effect where an absorption peak is observed when photons are forbidden from propagating because of high reflectivity.[26] The SiN TO and LO modes are associated with network vibrational modes and are sensitive to both film composition and film microstructure. Annealing of the $X_g = 0.05$ film (N doped Si film) enabled Lin and Lee to assign the shoulder at 780 cm^{-1} to the Si-N stretching mode in a HSi_2-Si-N, and the peak at 885 cm^{-1} to Si_2-NH. The 840 cm^{-1} peak is assigned to the vibration of the trigonal Si3N group either isolated in N doped aSi or in an extended SiN network which becomes IR active due to lattice disorder.[26,33,39]

The LO mode (900-1100 cm-1) is quite sensitive to changes in film composition.[26,28,35-40] As shown in Figure 1(a) as X_g is increased > 0.6, the intensity of the LO mode (900-1100 cm^{-1}) increases dramatically and shifts to higher frequencies. {*As this band could also be attributable to Si-O stretching of SiO_2 care must be exercised when assigning this band to ensure an oxygen free SiN film.}* In NH rich films, a lower intensity mode at 960-1020 cm^{-1} is attributed to vibration of a SiNxH cluster with H bonded to nitrogen. [26,28,32,35- 38] Tsu etal. describes a planar silicon dimide structure in which NH is

inserted between pairs of Si atoms in the same plane to form a planar Si-N(H)-Si linkage comparable to the Si-O-Si linkage in SiO_2 to account for this vibrational mode.[38] Annealing of the $X_g = 0.95$ film (NH rich a-SiN_x:H film) (Figure 2), resulted in the absorption at 980 cm^{-1} increasing in magnitude and shifting to 1070 cm^{-1}.[26] This is attributed to the elimination of hydrogen atoms and the transition from $SiNH_2$ structure to a denser Si_3N_4 network.[26,32,34,39,40] The blueshifting of the Si-N stretching absorption peak is attributed to shorter Si-N bond lengths and lower bond angles as hydrogen is eliminated from the film.[32,34] In Si rich, NH poor films annealing may also increase the absorption at 900-1100 cm^{-1}. This is attributed to annealing induced reordering which increases SiN_4 bonding and is correlated with the precipitation of silicon nanocrystals.[29,35]

As X_g increases the Si-H stretching-mode absorption upshifts or blue shifts from 2080 to 2180 cm^{-1}. This is attributed to the induction effect. Because the nitrogen atom is more electronegative than silicon, increasing the number of nitrogen atoms backbonded to Si-H causes the Si-H stretching mode to upshift to higher frequencies.[33,41] The Si-H (stretching absorption) may be deconvoluted into multiple bands arising from specific configurations H-Si-$Si(H)_{3-x}N_x$ which are summarized in the peak assignment table.[28,32,33]

As shown in Figure 1(b), as X_g increases, the N-H stretching mode at 3300 cm^{-1} and rocking mode at 1170 cm^{-1} and NH_2 bending mode at 1550 cm^{-1} increases while concurrently the Si-H stretching mode at 2100 cm^{-1} and Si-H rocking mode at 640 cm^{-1} decreases. This increasing NH/SiH ratio is indicative of increasing nitrogen content in the film and replacement of SiH bonds with NH bonds. The N-H (stretching) band near 3320 cm^{-1} is observed to be an asymmetric peak with a tail extending down to 2900 cm^{-1}. This asymmetry is partially due to hydrogen bonding between the H atoms in the N-H bonds and lone-pair electrons on nearby nitrogen atoms.[42,43] As the nitrogen content increases, the N-H stretching mode intensity increases, broadens and slowly shifts up from 3300 to 3350 cm^{-1}. This is attributed to the emergence of NH_2 which has symmetric and asymmetric stretching modes at 3280 and 3345 cm^{-1}, respectively.[43] This is consistent with the increasing intensity of NH_2 bending mode at 1550 cm^{-1}.

The concentration of hydrogen bonded to silicon or nitrogen may be estimated by the expression

$$[X\text{-}H] = A_{[X\text{-}H]} I_{[X\text{-}H]} \quad X = Si \text{ or } N \qquad (2)$$

where $A_{[X\text{-}H]}$ is an empirically determined proportionality coefficient and I is the integrated intensity of the SiH absorption at 2000-2200 cm^{-1} or NH absorption at ~3300 cm^{-1}. Various proportionality coefficients are reported from literature and are summarized in Table 2.[28,32,33, 44,45] Verlann etal. attributed the wide discrepancies in proportionality factors to compositional changes in the SiN films.[45] Intensity of the SiH or NH absorption is generally determined by integrating over the area of the absorption. However, significant errors in intensity may arise from the effects of coherent multiple reflections in multilayer samples which are dependent on film thickness and refractive index and are greater for thinner silicon rich nitride films.[33,46,47] Therefore, care must be taken in making quantative comparisions of NH and SiH bond concentrations in a-SiN_x:H films of varying thickness and refractive indexes. However, relative qualitative comparisons of SiH and NH bond densities is an invaluable method of assessing film composition, microstructure, and assessing the impact of processing conditions.

Deposition Chemistry: Direct $SiH_4 + NH_3$

Film properties covering a wide range of compositions and densities can be prepared by varying gas mixture, power, pressure, temperature. Gases utilized are typically SiH_4, NH_3, and/or N_2 as reactant gases and inert gases such as helium or argon. The reaction mechanism is complex because of the many ground state and excited species generated and extensive bond scrambling occurring in the plasma. The result is similar to an extremely high temperature process with a large number of possible gas and surface phase reaction pathways.

Smith and Alimonda etal. studied a NH_3-SiH_4 direct plasma glow discharge with mass spectrometry.[48] Mass spectrometric analysis revealed that disilane and the aminosilanes, $SiH_{4-n}(NH_2)_n$ to be the principal products of NH_3-SiH_4 plasma. Silane and ammonia must first dissociate in order to provide the precursors for disilane and aminosilane formation (eq 3 and eq 4).[49]

$$e + SiH_4 \longrightarrow SiH_3 + H + e \quad \textbf{(3)}$$

$$e + NH_3 \longrightarrow NH_2 + H + e \quad \textbf{(4)}$$

After dissociation of SiH_4 and ammonia, formation of tetra-aminosilane $Si(NH_2)_4$ and triaminosilane $Si(NH_2)_3$* forms via multiple aminations of SiH_{4-x} wherein NH_2 is attached to SiH_3 (eq 5).[50,51,52]

$$SiH_3 + NH_2 \longrightarrow SiH_2(NH_2) + H \quad \textbf{(5)}$$

Successive insertions of NH_2 into the complex continues to add amino groups and eliminate H, until reaching tetra-aminosilane $Si(NH_2)_4$ (eq 6).

$$SiH_n(NH_2)_{3-n} + NH_2 \longrightarrow SiH_{n-1}(NH)_{4-n} + H \quad \textbf{(6)}$$

With the exception of the final compound, the intermediate aminosilanes retain a dangling bond explaining their reactivity. The rate limiting step is generating sufficient density of NH_2. Film growth proceeds with adsorption of tetra- and tri-aminosilanes on the film surface, where they undergo chemical condensation towards stoichiometric Si_3N_4 with ammonia elimination (eq 7). A $Si(NH_2)_3$ radical adsorbs on a N site. Amino groups from neighboring $Si(NH_2)_3$ on surface react with each other to evolve NH_3, leaving a Si and N dangling to combine to develop the Si-N bond. Condensation proceeds as long as excess species can reach other and combine to release NH_3. No H evolution is involved in this surface reaction.

$$3Si(NH_2)_4 \longrightarrow Si_3N_4 + 8NH_3 \quad \textbf{(7)}$$

Rf power was observed to be the main determinant of gas phase product ratio. At low rf power disilane was main plasma product even with NH_3/SiH_4 ratio of 25/1. Disilane elimination and aminosilane formation was favored at higher power, greater NH_3/SiH_4 ratios, higher pressure and longer residence times.[53] Smith and Alimonda etal. proposed tri-aminosilane as the main depositing species for SiN film deposition, because of its close correlation with deposition rate.[48] This is consistent with deposition studies utilizing SiD_4 and ND_3 which determined that 80-90% of H(D) in the film originated from $NH(D)_3$ and not from $SiH(D)_4$.[38,43,54] Modeling results concur that aminosilane radicals are the main deposition precursors in silicon nitride deposition.[55]

A-SiN_x:H film composition can vary widely with deposition conditions from N doped amorphous Si to nitrogen rich silicon nitride. Experimentally, as rf power increases and NH_3/SiH_4 ratio increases, deposition rate increases, N-H content increase, Si-H content decreases, and refractive index decreases.[48,56] Too much ammonia can result in a decreased deposition rate which has been attributed saturation of the silane amines via overwhelming tetra-aminosilane formation $Si(NH_2)_4$.[48,56] Higher pressure increases deposition rates, by increasing precursor residence time allowing sufficient time for the amination reactions to occur as well as more time for deposition before reaction products are pumped away.[48,56] As deposition temperature is increased, deposition rate decreases, refractive index increases, and N-H decreases. Decreased N-H and increased refractive index are consistent with retention of Si

containing radicals and loss of amino species at elevated temperatures.[48,56] Conversely at low deposition temperatures elevated levels of N-H are observed in the film and refractive index is reduced which suggests preferred absorption of nitrogen containing radicals at low temperature.[48,56]

HF etch rates increase with increased NH_3/SiH_4 ratio, increased power, and lower deposition temperatures.[48,56] These same conditions decrease refractive index and increase NH in the film. The increased HF etch rate with decreased refractive index and increased NH is attributed to increased amino (NH_x) basic groups available for attack by acids and not necessarily related to increased film density.

Direct $SiH_4 + N_2$

Direct rf plasma growth with SiH4-N_2 proceeds via SiH_n radicals and N radicals reacting at growth surface to form a-SiN_x:H films.[57] The use of N_2 as a reactant gas instead of NH_3 helps increase the plasma density and reduces the amount of hydrogen in PECVD SiN. [57,58,59] In contrast to NH_3-SiH_4 chemistry, no Si-N precursors are observed in the glow discharge of N_2-SiH_4, only disilane and H_2 are observed.[57] Disilane formation occurs when sufficient power is applied to dissociate SiH_4 to SiH_n but not enough to dissociate N_2. SiH_4 is known to dissociate readily even at extremely low power densities.[57,60] The dissociated SiH_n may react with itself to form Si_2H_n by-products such as disilane. Under low power, disilane containing plasma conditions, the undissociated N_2 molecules do not react with the SiH*n*, but instead act as inert diluents. The result is low deposition rates, Si rich films with little N-H observed in FTIR and high refractive indexes.[57-61]

If the power is raised, N_2-N dissociation increases, resulting in increased deposition rate, increased N-H in film, and decreased refractive index consistent with increased N/Si ratio in the bulk of the film. At high rf power and high N_2/SiH_4 gas ratio, disilane is not observed and SiH_4 is consumed by reaction of SiH_m radicals with N atoms at the film surface and become incorporated into the film. Increasing power, increasing N_2/SiH_4 gas ratio results in increased deposition rates, N-H and reduced refractive index.[58-62]

Increasing deposition temperature resulted in decreased deposition rate, decreased N-H and decreased total hydrogen. The decreased deposition rate is attributed to diffusion and desorption of surface atoms.[58,59,62] At deposition temperatures < 250^{o}C, a large increase in total hydrogen, primarily as N-H is observed, with a subsequent large decrease in refractive index.[58,60,62] Excess excited nitrogen in the gas phase leads to the incorporation of N-H bonding groups in the films, possibly through the formation of N-H bonds in the gas phase. For very high concentrations of excited nitrogen, the hydrogen transfer reaction from Si-H bonds (in silane) to N-H bonds is preferred over Si-H incorporation, resulting in films with only N-H observed in the infrared spectra.[59]

Helium dilution has a significant influence on deposited film properties including decreased Si-H, increased N-H, decreased nitrogen contents and decreased total hydrogen content.[58,59,61] Helium dilution decreases residence time, and results in decreased Si-H and increased N-H in deposited films. The decreased SiH and increased NH is attributed to reduction in silane utilization and relative increase of excited nitrogen in the plasma with decreased residence time. [58,59,61,63] The relative increase in excited nitrogen may be due to the excitation of molecular nitrogen through metastable interactions[64] and/or by the reduction of the rate of collisional de-excitation of excited nitrogen with ground state nitrogen in the gas phase. The reduction in frequency of gas phase collisions shields the reactants from fragmentation and reduces the formation of polymeric silane species in the gas phase. The resulting low reactant concentration in the plasma after He dilution tends to minimize the role of gas phase reactions and leads to film growth conditions dominated by surface reactions.[58] The low mass of He minimizes momentum transfer to the surface and minimizes plasma induced damage to the film surface interface. He dilution results in a denser film with fewer impurities, less total hydrogen, and produces a high quality film structure. [58,59,61,63]

Step coverage is much worse in the SiH_4-N_2 process and this is attributed to the much higher sticking coefficients of the reactant radicals which minimizes surface diffusion. Conformality of

deposition into trenches is poor because the SiH_n and N radical species have high sticking coefficiencts and low surface mobilities.[57]

Pulsed Rf deposition of a-SiN_x:H

In pulsed radio frequency plasma deposition of a-SiN_x:H alloys from SiH_4-N_2, film characteristics are modified by adjusting the duty cycle of the pulsed rf power, while keeping N_2/SiH_4 gas mixture constant.[65] Deposition of rough, porous silicon rich nitride with large SiH content is observed as the duty cycle is decreased. Less energy per cycle is delivered to the plasma which reduces the amount of dissociated SiH_3 and N* radicals for film growth. As the duty cycle is reduced, the concentration of N* radicals decreases faster than SiH_3 radicals resulting in lower N/SiH_3 gas phase ratio and deposition of silicon rich nitride films. Ion bombardment of the surface is reduced; energetic ions arrive at the surface only during pulse on, while radicals created within the pulse and diffusing from gas phase to surface during pulse off have low energy, reducing the overall mean energy per deposited particle decreases with reduced duty cycle. The reduced mean particle energy decreases ion induced surface mobility and ion knock in effects leading to increased SiH hydrogen content, increased porosity and higher roughness. Roughness was found to strongly depend on duty cycle from 100% to 40% roughness increased because of lower ion bombardment at surface. As duty cycle was reduced less than 40%, roughness decreased as the decrease of ion bombardment was counterbalanced by enhanced surface diffusion.

Indirect SiH_4 + NH_3, He, Ar

Remote plasma enhanced chemical vapor deposition (RPECVD) of silicon nitride can be viewed as a four stage process, (1) rf excitation of a gas or gas mixture that contains nitrogen atoms including N_2 or NH_3, (2) transport of excited species out of plasma region, (3) reaction of transported species with silicon reactant typically SiH_4, and (4) deposition of film by CVD process onto a heated substrate. RPECVD of SiN from SiH_4-NH_3, by analogy shares similar growth mechanism as direct SiH_4-NH_3 with formation of aminosilanes[48-56] from interactions of activated NH_2 and NH with silane radicals.[66,67] Kushner modeled rare gas-silane-ammonia mixtures and concluded that NH_2 radicals are dominantly produced by excitation transfer from activated rare gases (Rg = He, Ar) eq 8 and electron impact eq 8.[52] Because ammonia is unreactive with hydrogen and silane at moderate gas temperatures, production of NH_2 by H abstraction from NH_3 or reaction with SiH_4 is not significant.[49]

$$Rg^* + NH_3 \longrightarrow NH_2 + Rg \quad (8)$$

$$e + NH_3 \longrightarrow NH_2 + H + e \quad (9)$$

SiH_3 radicals are produced dominantly by excitation transfer eq 10 and hydrogen abstraction reactions eq 11.

$$Rg^* + SiH_4 \longrightarrow SiH_3 + H + Rg \quad (10)$$

$$H + SiH_4 \longrightarrow SiH_3 + H_2 \quad (11)$$

The source of H in the abstraction reaction (11) is likely the excitation transfer (10) or reactions that generate NH_2 such as eq 8 or 9. Generating a single NH_2 radical will with high probability generate both reactants required to form an amino-silane complex, consequently the rate limiting step is the production of NH_2.[49] As in direct PECVD, for RPECVD with SiH_4-NH_3, $NH(D)_3$ is the hydrogen source not SiH_4.[67] Growth rate increases with increasing NH_3 flow.[66]

At low deposition temperatures (100°C), the a-SiN_x:H film contains large amounts of NH and is considered an alloy of silicon nitride and silicon diimide with a refractive index of 1.75 intermediate between Si_3N_4 and SiO_2.[54] Silicon diimide is an isoelectronic analog of SiO_2 in which each oxygen atom is replaced with $Si(NH_2)$.[38] Increasing the deposition temperature, decreases N-H in the film, and

increases the refractive index. Increasing He or Ar dilution decreases N-H in the film and decreases the deposition rate by reducing the probability of radical-radical reactions.[54]

In an expanding thermal plasma (ETP) growth with SiH_4-NH_3 with argon dilution, N incorporation proceeds via surface reactions of impinging NH_2 and N radicals inserting into Si-Si backbonds of a-Si:H like layer created by impinging SiHx radicals. Formation of aminosilanes was not observed and was attributed to the relatively high atomic hydrogen from dissociative recombination reactions of NHx with electrons eq 7and short residence time in ETP.[68]

Indirect $SiH_4 + N_2$, He, Ar

RPECVD with SiH_4-N_2 proceeds via SiH_3 radicals and N radicals reacting at growth surface to produce a-SiN_x:H as postulated for SiH_4-N_2 direct rf plasma growth.[54,63,69,70] Hydrogen in the deposited films is primarily incorporated as Si-H, because the N radical flux is low.[54] As power is increased, SiH decreases, and NH increases while overall hydrogen decreases. We would expect the flux of Si and N radicals to increase with power, however, formation of the N radical is the rate limiting step and its flux to the surface increases faster than the SiH_n flux.[66] Helium dilution increases growth rate and Si-H in film. He dilution of N_2 discharges is known to reduce deexcitation reactions between excited N atoms N* and N_2 molecules. The increased growth rate is attributed to a higher N* flux and therefore to rates increased precursor formation and surface interaction.[71] Argon dilution decreased the growth rate, decreased refractive index and increased N-H in film. Decreased growth rate in SiH_4 - N_2 - Ar system is attributed to decreased concentration of silane radicals from dissociation of SiH_4 from collisions with excited molecules because of the lower electron concentration in argon nitrogen discharge, because argon is more difficult to excite. Decreased refractive index and increased N-H is attributed to greater nitrogen incorporation. An enhanced atomic nitrogen formation and thus a larger activated nitrogen flux to the surface is promoted by argon dilution by enabling selective direct excitation of molecular nitrogen by argon atoms in metastable electronic states.[72]

Stress

Stress in a-SiN_x:H films deposited by PECVD films can be generated by modifying major process parameters.[19,73,74,75] The main deposition parameter affecting stress is substrate bias frequency. High frequency benefits tensile stress, while low frequency rf (400 kHz) has been observed to induce compressive stress in PECVD SiN films. Tensile stress typically arises in PECVD a-SiN_x:H films grown with SiH_4 and NH_3 and increases with increased RF frequency, decreased power, increased deposition pressure, increased deposition temperature and thermal anneals at temperatures above the deposition temperature. Tensile stress is theorized to result from the elimination reactions (eq 12 and 13) which form the film[49] and which occur during annealing.[76]

$$Si\text{–}H + H\text{–}NSi\text{–}H \rightarrow Si - Si + NH_3 \quad (12)$$

$$Si\text{–}H + N - H \rightarrow Si - N + H_2 \quad (13)$$

As shown in Figure 3, during deposition, film densification is proposed to occur in a chemical condensation zone which extends beneath the film surface. Elimination of volatile species (ammonia, hydrogen) from this region generates dangling bonds which have limited degrees of freedom because they are constrained by the existing SiN network. Si-N bond formation occurs over voids resulting in generation of tensile stress from the “stretched” bond.[49]

Compressive stress typically arises in PECVD a-SiN_x:H films grown with SiH_4 and N_2 and increases at lower rf frequencies, lower deposition temperatures, lower pressures, and greater power. Compressive stress is induced by positive incorporation during deposition. Ion bombardment during deposition increases compressive stress by energetic expansion of the surface layer and incorporation of positive ions either Ar^+, N_2^+, H^+, or N^+.[53,62,72,] As shown in Figure 4, incorporation of ions in the lattice spaces squeezes or compresses the network together. The probability of incorporating bonding ions such as H^+ or N^+ can be promoted by low surface field because of large sticking coefficient. At higher frequencies above 4 MHz the ions become slow compared to the oscillating frequency leading to a decrease in the ion bombardment energy and the flux of ions to the electrode. The ion bombardment effect of the low frequency component densifies SiN film and produces denser, more compressive films, whereas high frequency alone usually produces tensile films. Multilayer SiN structures generated by maintaining a N_2 plasma but cycling SiH_4 and ammonia have been demonstrate to increase both compressive and tensile stress compared to a SiN film deposited without interruption as a single layer.[19,20]

The FTIR spectra of compressive and tensile films show significant differences.[19] Both films exhibit NH_x stretching and bending modes, but the compressive film has overall higher NH_x stretching intensity. Additionally, the compressive film shows significantly higher SiH and SiN bonding than the tensile film. Compressive PECVD films typically have more bonded hydrogen than tensile films, and the most tensile films have the lowest amount of bonded hydrogen combination of NH_x and SiH.

Conclusion

Amorphous hydrogenated silicon nitride (a-SiN_x:H) materials prepared by plasma-enhanced chemical vapor deposition (PECVD) are of high interest because of their suitability for diverse applications in many fields including microelectronics, photovltaics, and photonics. A summary of the FTIR assignments from literature is described. PECVD a-SiN_x:H film composition can vary widely with deposition conditions from N doped amorphous Si to nitrogen rich silicon nitride. Film properties covering a wide range of compositions and densities can be prepared by varying gas mixture, power, pressure, temperature. PECVD a-SiN_x:H grown with SiH_4 and NH_3 proceeds via formation of aminosilanes and tends to have a larger hydrogen content and have tensile stress. PECVD a-SiN_x:H grown with SiH_4 and N_2 proceeds via incorporation of SiH3 and N radicals at the film surface and tends to have a lower hydrogen content, be less conformal and be compressively stressed.

References

[1] A. H. White , W. Melville, The Decomposition of Ammonia at High Temperatures. J. Am. Chem. Soc., 1905, 27 (4), 373.

[2] S. Wolf and R. N. Tauber, Silicon Processing for the VLSI Era–Vol 1. Process Technology ~Lattice, Sunset Beach, 1986, p. 192.

[3]J. Osenbach and S. Voris, Sodium diffusion in plasma-deposited amorphous oxygen-doped silicon nitride (a-SiON:H) films J. Appl. Phys. 63 4494 (1988)

[4] R.K. Ulrich, A.J. Phillips, D.H. Yi, W.D. Brown, S.S. Ang, Mechanical stability of PECVD silicon nitride protective films over bondwires, bonds and bondpads during thermal stress. Microelectronics Reliability 31, 1237, 1991.

[5] D.S. Wuua, W.C. Loa, C.C. Chianga, H.B. Lina, L.S. Changa, R.H. Horngb, C.L. Huangc, Y.J. Gaoc, Water and oxygen permeation of silicon nitride films prepared by plasma-enhanced chemical vapor deposition, Surface and Coatings Technology, 198, 114 2005.

[6]C. Headley, L. Fu, P. Parkinson, X. Xu, J. Lloyd-Hughes, C. Jagadish, M. B. Johnston, Improved Performance of GaAs-Based Terahertz Emitters via Surface Passivation and Silicon Nitride Encapsulation IEEE Journal of Selected Topics in Quantum Electronics, 17, 17, 2011.

[7] Gatabi, I.R.; Johnson, D.W.; Jung Hwan Woo; Anderson, J.W.; Coan, M.R.; Piner, E.L.; Harris, H.R., "PECVD Silicon Nitride Passivation of AlGaN/GaN Heterostructures," Electron Devices, IEEE Transactions on , vol.60, no.3, pp.1082,1087, March 2013

[8] Chang, Edward Y.; Cibuzar, G.T.; Pande, K.P., "Passivation of GaAs FET's with PECVD silicon nitride films of different stress states," Electron Devices, IEEE Transactions on , vol.35, no.9, pp.1412,1418, Sep 1988

[9] D. R. Cote, S. V. Nguyen, W. J. Cote, S. L. Pennington, A. K. Stamper, D. V. Podlesnik, Low temperature chemical vapor deposition processes and dielectrics for microelectronic circuit Manufacturing at IBM. IBM J. Res. Develop. 39, 437, 1995

[10] A.S. Lee, N. Rajagopalan, M. Le, B.H. Kimand, H. M'Saad, Development and Characterization of a PECVD Silicon Nitride for Damascene Applications, J. Electrochem. Soc. volume 151, F7-F9 2004

[11] G. Oversluizen, W.H.M. Lodders, I.D. French Plasma-enhanced chemical vapour deposition of amorphous silicon nitride for thin film diode active matrix liquid crystal displays Thin Solid Films, 241 287, 1994.

[12] N. Lustig and J. Kanicki ,Gate dielectric and contact effects in hydrogenated amorphous silicon - silicon nitride thin film transistors J Appl Phys 65 3951 (1989)

[13] Y. Park, S.Ree, Bulk and Interface Properties of low-temperature silicon nitride films deposited by remote plasma chemical vapor deposition. J. Materials Science: Materials in Electronics 12, 515, 2001

[14] Y. Kuo PECVD Nitride as a Gate Dielectric for Amorphous Silicon Thin Film Transistor. J. Electrochem. Soc. 142 186 (1995)]

[15]W. Zhu, D. Neumayer, V. Perebeinos, and P. Avouris, Silicon Nitride Gate Dielectrics and Band Gap Engineering in Graphene Layers. *Nano Lett.*, *10*, 3572, 2010.

[16] A. Kshirsagara, P. Nyaupanea, D. Bodasc, S.P. Duttaguptaa, S.A. Gangal, Deposition and characterization of low temperature silicon nitride films deposited by inductively coupled plasma CVD, Applied Surface Science 257 (2011) 5052

[17] H Huang, K Winchester, Y Liu, X Z Hu, C A Musca, J. M. Dell, L. Faraone, Determination of mechanical properties of PECVD silicon nitride thin films for tunable MEMS Fabry–Perot optical filters. J. Micromech. Microeng. 15 (2005) 608–614

[18] A Tarraf, J Daleiden, S Irmer, D Prasai, H Hillmer, Stress investigation of PECVD dielectric layers for advanced optical MEMS. J. Micromech. Microeng. 14 (2004) 317–323

[19] M. Belyansky, M. Chace, O. Gluschenkov, J. Kempisty, N. Klymko, A. Madan, A. Mallikarjunan, S. Molis, P. Ronsheim, Y. Wang, D. Yang, and Y. Li, Methods of producing plasma enhanced chemical vapor deposition silicon nitride thin films with high compressive and tensile stress. J. Vac. Sci. Technol. A 26, 517 2008.

[20] Yang, H. S.; Malik, R.; Narasimha, S.; Li, Y.; Divakaruni, R.; Agnello, P.; Allen, S.; Antreasyan, A.; Arnold, J.C.; Bandy, K.; Belyansky, M.; Bonnoit, A.; Bronner, G.; Chan, V.; Chen, X.; Chen, Z.; Chidambarrao, D.; Chou, A.; Clark, W.; Crowder, S.W.; Engel, B.; Harifuchi, H.; Huang, S.F.; Jagannathan, R.; Jamin, F.F.; Kohyama, Y.; Kuroda, H.; Lai, C. W.; Lee, H.K.; Lee, W-H; Lim, E. H.; Lai, W.; Mallikarjunan, A.; Matsumoto, K.; McKnight, A.; Nayak, J.; Ng, H. Y.; Panda, S.; Rengarajan, R.; Steigerwalt, M.; Subbanna, S.; Subramanian, K.; Sudijono, J.; Sudo, G.; Sun, S.-P.; Tessier, B.; Toyoshima, Y.; Tran, P.; Wise, R.; Wong, R.; Yang, I.Y.; Wann, C.H.; Su, L.T.; Horstmann, M.; Feudel, Th; Wei, A.; Frohberg, K.; Burbach, G.; Gerhardt, M.; Lenski, M.; Stephan, R.; Wieczorek, K.; Schaller, M.; Salz, H.; Hohage, J.; Ruelke, H.; Klais, J.; Huebler, P.; Luning, S.; van Bentum, R.; Grasshoff, G.; Schwan, C.; Ehrichs, E.; Goad, S.; Buller, J.; Krishnan, S.; Greenlaw, D.; Raab, M.; Kepler, N., "Dual stress liner for high performance sub-45nm gate length SOI CMOS manufacturing," Electron Devices Meeting, 2004. IEDM Technical Digest. IEEE International , vol., no., pp.1075,1077, 13-15 Dec. 2004

[21] H. Mackel, R. Ludemann, Detailed Study of the composition of hydrogenated SiNx layers for high-quality silicon surface Passivation. J. Appl. Phys. 92, 2602 2002.

[22] F. Duerinckx, J. Szlufcik Defect passivation of industrial multicrystalline solar cells based on PECVD silicon nitride Solar Energy Materials & Solar Cells 72, 231 2002.

[23] Y. Wan, K.R. McIntosh, A.F. Thomson, Characterisation and Optimisation of PECVD SiNx as an antireflection coating and passivation layer for silicon solar cells. AIP Advances 3, 032113, 2013

[24] H. Schlemm, A. Mai[a], S. Roth[a], D. Roth, K.-M. Baumgärtner[b], H. Muegge Industrial large scale silicon nitride deposition on photovoltaic cells with linear microwave plasma sources. Surface and Coatings Technology 174–175, 2003, 208

[25] W. Soppe, H. Rieffe, A. Weeber, Bulk and Surface Passivation of Silicon Solar Cells Accomplished by Silicon Nitride Deposited on Industrial Scale by Microwave PECVD. Progress in Photovoltaics: Research and Applications, 13, 551, 2005.
[26] K. Lin and S. Lee, The structural and optical properties of aSiNx:H prepared by plasma enhanced chemical vapor deposition, J. Appl. Phys. 72, 5474 (1992)
[27] G. Lucovsky, J. Yang, S.S. Chao, J.E. Tyler, W. Czubatyj, Nitrogen-bonding environments in glow-discharge-deposited a-Si:H films, Physical Review B, 28, 3234, 1983.
[28] E. Bustarret, M. Bensouda, M. C. Habrard, J. C. Bruyere, S. Poulin, S. C. Gujrathi, Configurational statistics in a-Si, Ny H, alloys: A quantitative bonding analysis, Physical Review B 38 8171, 1988
[29] G. Scardera, T. Puzzer, G. Conibeer, M.A. Green, Fourier transform infrared spectroscopy of annealed silicon-rich silicon nitride thin films, J. Appl. Phys. 104, 104310, 2008.
[30] J. Bandet, B. Despax, M. Caumont, Nitrogen bonding environments and local order in hydrogenated amorphous silicon nitride films studied by Raman spectroscopy, J. Appl. Phys. 85, 7899 (1999)
[31] F. Demichelis, F. Giorgis, C.F. Pirri, Compositional and structural analysis of hydrogenated amorphous silicon – nitrogen alloys prepared by plasma-enhanced chemical vapour deposition. Philosophical Magazine B, 74, 155 (1996).
[32] S. Hasegawa, L. He, Y. Amano, and T. Inokuma, Analysis of SiH and SiN vibrational absorption in amorphous SiN_x:H films in terms of a charge-transfer model, Phys. Rev. B 48, 5315–5325 (1993)
[33] M.H. Brodsky, M. Cardona, J.J. Cuomo, Infrared and Raman spectra of the silicon-hydrogen bonds in amorphous silicon prepared by glow discharge and sputtering, Phys. Rev. B 16, 3556, 1977
[34] J. J. Mei, H. Chen, and W. Z. Shen, H. F. W. Dekkers, Optical properties and local bonding configurations of hydrogenated amorphous silicon nitride thin films, J. Appl. Phys. 100, 073516 (2006)
[35] O. Debieu, R. P. Nalini, J Cardin, X. Portier, J. Perrière, F. Gourbilleau, Structural and optical characterization of pure Si-rich nitride thin films, Nanoscale Research Letters 2013, 8:31
[36] T. Li, J. Kanicki, Observation of incident angle dependent phonon absorption in hydrogenated amorphous silicon nitride thin films, Appl. Phys. Lett. 73, 3866. (1998).
[37] G. DuPont, H. Caquineau, B. Despax, R. Berjoan, A. Dollet, Structural Properties of N-rich a-Si-N:H films with a low electron trapping rate, J. Phys. D: Appl. Phys. 30, 1064 (1997).
[38] D.V. Tsu, G. Lucovsky, M.J. Mantini, Local atomic structure in thin films of silicon nitride and silicon diimide produced by remote plasma-enchanced chemical-vapor deposition, Phys. Rev. B, 33, 7069 (1986).
[39]D.Della Sala, C Coluzza, G Fortunato, F Evangelisti, Infrared and optical study of a-SiN alloys, Journal of Non-Crystalline Solids, 77–78, 933, (1985).
[40] M. Ippolito and S. Meloni Atomistic structure of amorphous silicon nitride from classical molecular dynamics simulations Phys. Rev. B 83, 165209 (2011)
[41] G.N Parsons, G. Lucovsky, Silicon-hydrogen bond-stretching vibrations in hydrogenated amorphous silicon-nitrogen alloys, Physical Review B, 41, 1664, 1990.
[42] Z. Yin, F.W. Smith Optical dielectric function and infrared absorption of hydrogenated amorphous silicon nitride films: Experimental results and effective-medium-approximation analysis, Physical Review B, 42, 3666, 1990.
[43] M. Maeda, H. Nakamura, Infrared Spectroscopic study of hydrogenated and deutrated silicon nitride films prepared from plasma enhanced deposition, J. Appl. Phys. 55, 3068, (1984).
[44] W.A. Lanford and M.J. Rand, The hydrogen content of plasma - deposited silicon nitride J. Appl. Phys. 49**,** 2473 (1978)
[45] V. Verlaan, C. H. M. van der Werf, W. M. Arnoldbik, H. D. Goldbach, and R. E. I. Schropp, Unambiguous determination of Fourier-transform infrared spectroscopy proportionality factors: The case of silicon nitride, Phys. Rev. B 73, 195333 (2006).
[46] A. A. Langford, M. L. Fleet, and B.P. Nelson, W. A. Lanford, N. Maley, Infrared absorption strength and hydrogen content of hydrogenated amorphous silicon, Phys Rev. B, 45, 13372, (1992).
[47] N. Maley, Critical investigation of the infrared-transmission-data analysis of hydrogenated amorphous silicon alloys, Phys. Rev. B, 46, 2078 (1992).
[48] D.L. Smith, A.S. Alimonda, C.C. Chen, S.E. Ready, B. Wacker, J. Vac. Sci. Technol. B, Mechanism of SiNxHy deposition from NH_3-SiH_4 Plasma. J. Electrochem. Soc. 137, 614, 1990
[49] D.L. Smith, Controlling the Plasma Chemistry of Silicon Nitride and Oxide Deposition from Silane. J. Vac. Sci. Technol. A 11, 1843, 1993.

[50] D. B. Beach and J. M. Jasinski, Excimer Laser Photochemistry of Silane-Ammonia Mixtures at 193 nm. Journal of Physical Chemistry, 94, 3019, 1990

[51] J.L. Guizot, P. Alnot, F. Wyczisk J. Perrin, B. Allain, Kinetics of deposition and electrical properties of silicon nitride films obtained by 185 nm photolysis of SiH_4–NH_3 mixtures Semicond. Sci. Technol. 6 582–9 1991

[52] M.J. Kushner, Simulation of the Gas-phase Processes in remote-plasma-activated chemical-vapor deposition of silicon dielectrics using rare gas silane ammonia mixtures. J. Appl. Phys. 71, 4173, 1992.

[53] D.T. Murley, R.A.G. Gibson, B. Dunnett, A. Goodyear, I.D. French, Influence of gas residence time on the deposition of nitrogen-rich amorphous silicon nitride Journal of Non-Crystalline Solids 187 (1995) 324

[54] D.V. Tsu, G. Lucovsky, Silicon Nitride and Silicon diimide grown by remote plasma enhanced chemical vapor deposition, J. Vac. Sci. Technol. A, 4, 480 (1986).

[55] M. Bavafa, H. Ilati, B. Rashidian, Comprenhensive Simulation of the effects of process conditions on plasma enhanced chemical vapor deposition of silicon nitride. Semiconductor Science and Technology 23, 095023 2008.

[56] T.J. Cotler, J. Chapple-Sokol, High Quality Plasma-Enhanced Chemical Vapor Deposited Silicon Nitride Films, J. Electrochem. Soc. 140, 2071, 1993.

[57] D.L. Smith, A.S. Alimonda, F.J. von Pressing, Mechanism of SiNxHy deposition from N_2-SiH_4 Plasma J. Vac. Sci. Technol. B,. 8, 551, 1990.

[58] T.M. Klein, T.M. Anderson, A.I. Chowdhury, G.N. Parsons, Hydrogenated silicon nitride thin films deposited between 50 and 250^{o}C using nitrogen/silane mixtures with helium dilution. J. Vac. Sci. Technol. A. 17, 108, 1999.

[59] T. Karabacak, Y.P. Zhao, G.C. Wang, T.M. Lu, Growth front roughening in silicon nitride films by plasma-enhanced chemical vapor deposition Physical Review B 66, 075329 2002

[60] F. Kampas and R. Griffith, Origin of emitting species in the plasma deposition of aSi:H alloys J. Appl. Phys. 52 (1981) 1285.

[61] G.N. Parsons, J.H. Souk, J. Batey, Low hydrogen content stoichiometric silicon nitride films deposited by plasma-enhanced chemical vapor deposition, J. Appl. Phys. 70, 1553 (1991).

[62] H. Dun, P. Pan, F.R. White, R.W. Douse, Mechanisms of Plasma-Enhanced Silicon Nitride Deposition using SiH_4/N_2 Mixture. J. Electrochem. Soc. 128, 1555, 1981.

[63] A. I. Chowdhury, T. M. Klein, T. M. Anderson, and G. N. Parsons, Silane consumption and conversion analysis in amorphous silicon and silicon nitride plasma deposition using in situ mass spectroscopy, J. Vac. Sci. Technol. A 16, 1852 (1998)

[64] Chorng Lieh Lin and Frederick Kaufman, Reactions of Metastable Nitrogen Atoms, J. Chem. Phys. 55, 3760 (1971)

[65] R. Vernhes, O. Zabeida, J.E. Klemberg-Sapieha, L. Martinu, Pulsed radio frequency plasma deposition of a-SiNx:H alloys: Film properties, growth mechanism, and applications. J. Appl. Phys. 100 063308 (206).

[66] J.A. Theil, S.V. Hattangady, G. Lucovsky, Effects of NH_3 and N_2 source gases and plasma excitation frequencies on the reaction chemistry for Si_3N_4 thin-film growth by remote plasma-enhanced chemical vapor deposition, J. Va. Sci. Technol. A 10, 719 (1992).

[67] Z. Lu, P. Santos-Filho, G. Stevens, M.J. Williams, G. Lucovsky, Fourier transform infrared study of rapid thermal annealing of a-Si:N:H(D) films prepared by remote plasma chemical vapor deposition, J. Vac. Sci Technol. A 13, 607 (1995).

[68] P. J. van den Oever, J. H. van Helden, J. L. van Hemmen, R. Engeln, D. C. Schram N, NH, and NH2 radical densities in a remote Ar–NH_3–SiH_4 plasma and their role in silicon nitride deposition, J. Appl. Phys. 100, 093303 (2006);

[69] W. M. M. Kessels, F. J. H. van Assche, J. Hong, D. C. Schram, and M. C. M. van de Sanden Plasma diagnostic study of silicon nitride film growth in a remote Ar–H_2–N_2–SiH_4 plasma: Role of N and SiH_n radicals, J. Vac. Sci. Technol. A 22, 96 (2004)

[70] B.F. Hanyaloglu, E.S. Aydil, Low temperature plasma deposition of silicon nitride from silane and nitrogen plasmas, J. Vac. Sci. Technol. A, 16, 2794, (1998).

[71] D.V. Tsu, G. Lucovsky, Silicon Nitride and Silicon diimide grown by remote plasma enhanced chemical vapor deposition, J. Vac. Sci. Technol. A, 4, 480 (1986).

[72] S.E. Alexandrov, Remote PECVD: a route to controllable plasma deposition. J. de Physique IV, Colloque C5, 567 (1995).

[73] W. A. P. Claassen W. G. J. N. Valkenburg, M. F. C. Willemsen, W. M. v. d. Wijgert, Influence of Deposition Temperature, Gas Pressure, Gas Phase Composition, and RF Frequency on Composition and Mechanical Stress of Plasma Silicon Nitride Layers J. Electrochem. Soc. 1985 volume 132, issue 4, 893-898

[74] R. Agravani, L. Xia, H. M'Saad, G. Karunasiri, A. Mascarenhas, and S. E. Thompson, A reliable and manufacturable method to induce a stress of >1 GPa on a P-channel MOSFET in high volume manufacturing IEEE Electron Device Lett. 27, 114 (2006)

[75] W. A. P. Claassen, Ion bombardment-induced mechanical stress in plasma-enhanced deposited silicon nitride and silicon oxynitride films, Plasma Chemistry and Plasma Processing 1987, 7, 109.

[76] F.L. Martinez, A. del Prado, I. Martil, G. Gonzalez-Diaz, Molecular models and activation energies for bonding rearrangement in plasma-deposited *a*-SiN_x:H dielectric thin films treated by rapid thermal annealing, Phys. Rev. B 63, 245320 (2001)

Figures

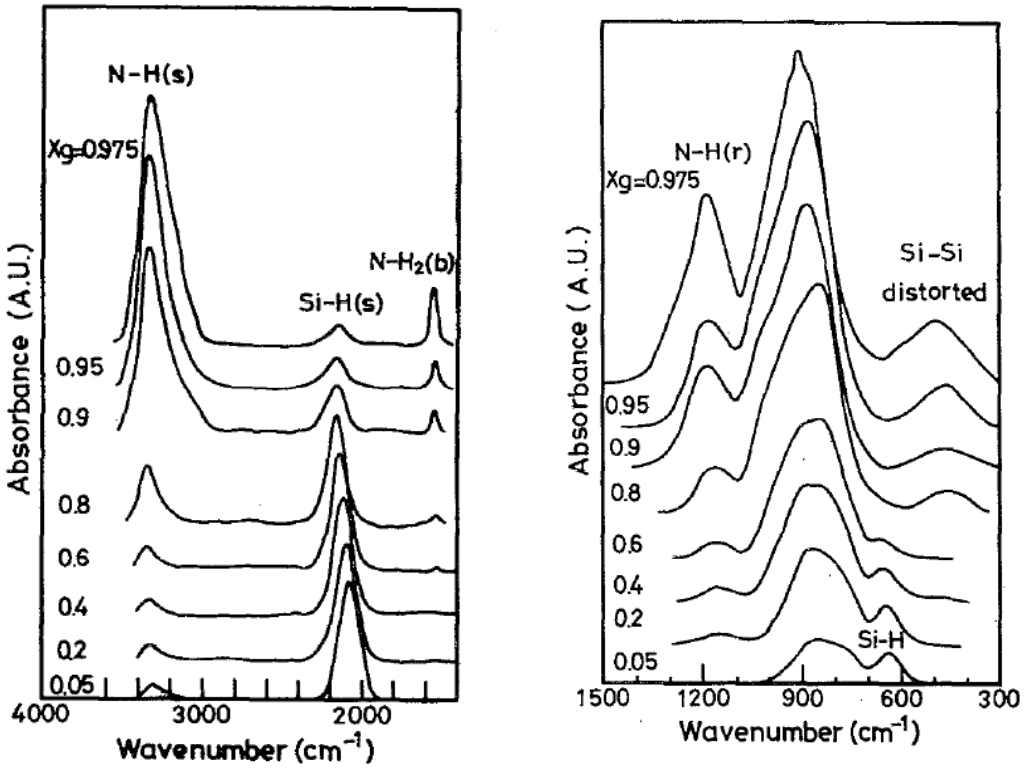

Figure 1. IR spectra of a-SiNx:H with different x, at a deposition temperature of 250°C with wave numbers between (a) 4000 and 1500 cm^{-1} and (b) 1500 and 300 cm^{-1}.

K. Lin and S. Lee, The structural and optical properties of aSiNx:H prepared by plasma enhanced chemical vapor deposition, J. Appl. Phys. 72, 5474 (1992)

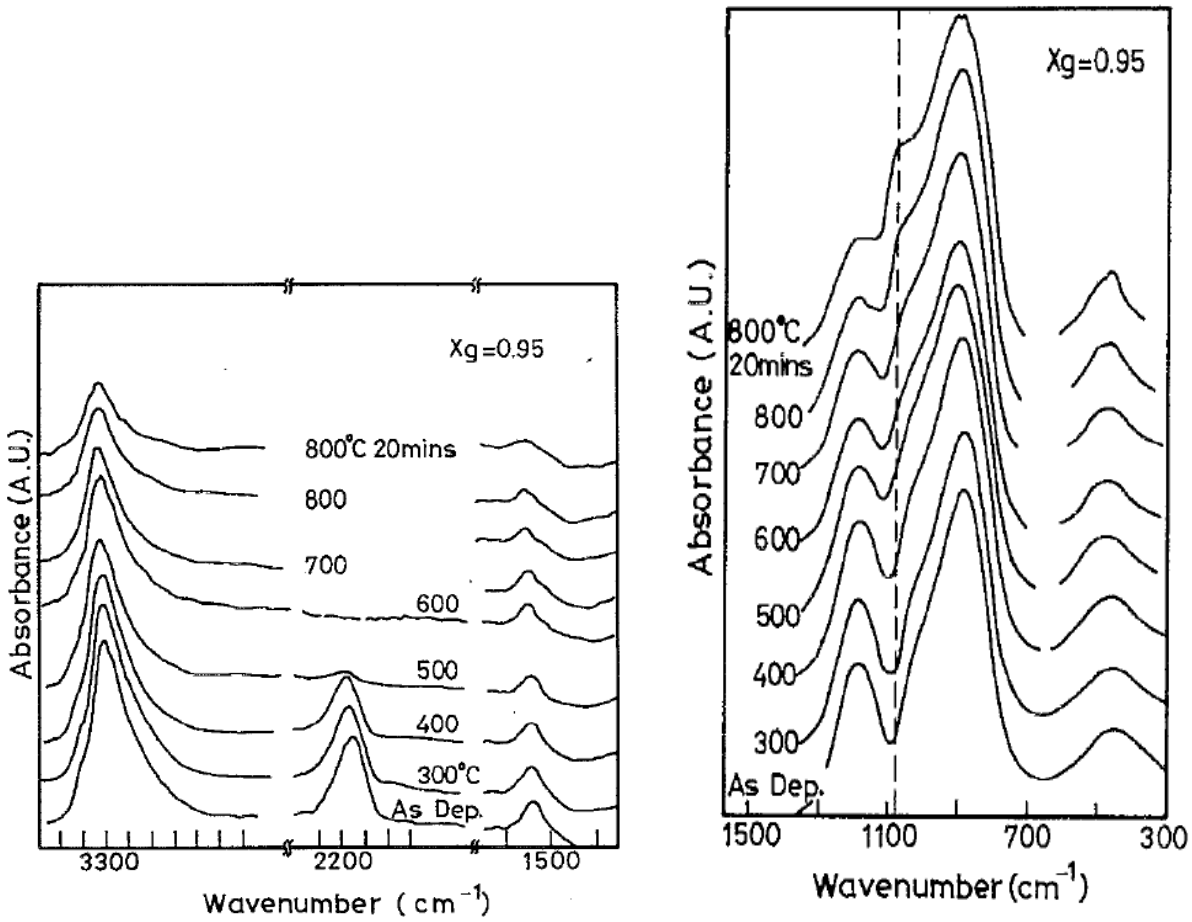

Figure 2. IR-absorption spectra of o-SiN;H deposited at 250°C with X_g=0.95 annealed at different temperatures with wave numbers between (a) 300 and 1500 cm-' and (b) 1400 and 4000 cm-'.

K. Lin and S. Lee, The structural and optical properties of aSiNx:H prepared by plasma enhanced chemical vapor deposition, J. Appl. Phys. 72, 5474 (1992)

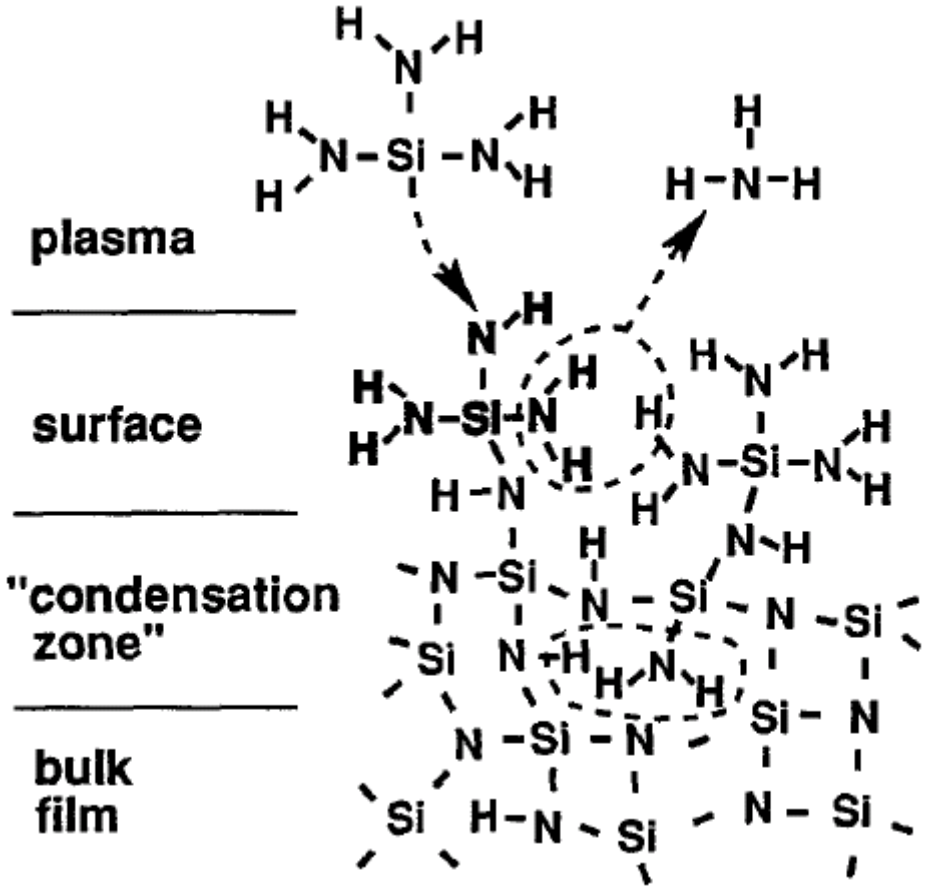

Figure 3. Cross-sectional model of the condensation of adsorbed $Si(NH_2)_3$ toward a Si-N network with evolution of NH_3.

D.L. Smith, A.S. Alimonda, C.C. Chen, S.E. Ready, B. Wacker, J. Vac. Sci. Technol. B, Mechanism of SiNxHy deposition from NH_3-SiH_4 Plasma. J. Electrochem. Soc. 137, 614, 1990

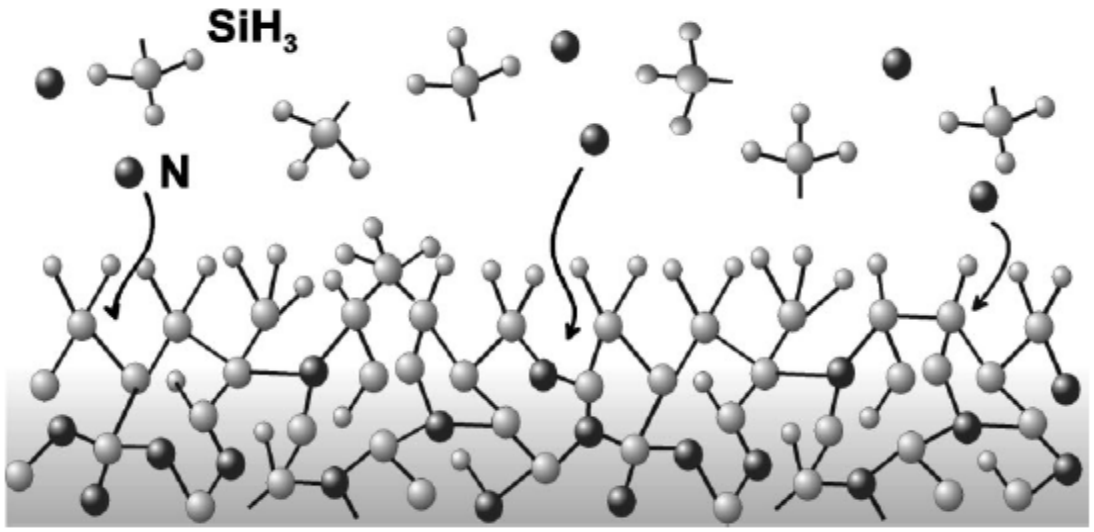

Figure 4. Schematic ball-and-stick model of the proposed *a*-SiN*x* :H growth mechanism from a N2 /SiH4 plasma.

W. M. M. Kessels, F. J. H. van Assche, J. Hong, D. C. Schram, and M. C. M. van de Sanden Plasma diagnostic study of silicon nitride film growth in a remote $Ar–H_2–N_2–SiH_4$ plasma: Role of N and SiH_n radicals, J. Vac. Sci. Technol. A 22, 96 (2004)

Table 1. Vibrational frequencies

bonding group	Frequency cm^{-1}	Configuration	motion	comments
Si-N	480	N-Si_3	symmetric stretching	arises from disruption of Si-Si network, increases with nitrogen
Si-N	780	HSi_2-Si-N	asymmetric stretch	isolated Si-N bond with H neighbor
Si-N	840	NSi_3	asymmetric stretch	TO mode of SiN assymetric stretch
Si-N	900-1000	Si-N(H)-Si	asymmetric stretch	LO mode of SiN assymetric stretch, increases and upshifts with NH
Si-N	1000-1100	SiN_4	symmetric stretching	LO mode of SiN assymetric stretch, increases with H elimination and film ordering
Si-H	630	HSi-Si_3	rocking	decreases and upshifts with nitrogen
Si-H	2005	HSi-Si_3	stretch	
Si-H	2065	H_2Si-Si_2	stretch	
Si-H	2082	HSi-NSi_2	stretch	
Si-H	2140	H-SiN_2Si, H_2SiNSi	stretch	
Si-H	2175	H_2SiN_2	stretch	
Si-H	2180	H-Si(SiN_2)	stretch	
Si-H	2220	H-SiN_3	stretch	
N-H	1175	Si-N(H)-Si	bend	increases with nitrogen
N-H2	1550	Si-$N(H)_2$-Si	bending	increases with nitrogen
N-H2	3280	Si-$N(H)_2$-Si	symmetric stretch	increases with nitrogen
N-H	3320	Si-N(H)-Si	symmetric stretch	increases with nitrogen
N-H2	3345	Si-$N(H)_2$-Si	asymmetric stretch	increases with nitrogen
H···N	< 3300 tail	N-H···N	hydrogen bonding	hydrogen bonding NH with N lone pairs

Table 2. FTIR proportionality factors 10^{19} (cm^{-2}) for different SiNx compositions.

		Verlaan		Bustarret		Lanford		Hasegawa
N/Si	Density	SiH	NH	SiH	NH	SiH	NH	SiH
	(g/cm^3)	10^{19} (cm^{-2})	10^{19} (cm^{-2})	10^{19} (cm^{-2})	10^{19} (cm^{-2})	10^{19} (cm^{-2})	10^{19} (cm^{-2})	10^{19} (cm^{-2})
1.35	2.03	12	18	20	12	14	28	4.8
1.24	2.62	10	25	28	12	14	28	5
1.2	2.93	5.5	47	30	12	14	28	5.2
1.09	2.71	16	25	36	12	14	28	5.5